Chromatin remodeling of the interleukin-2 gene: distinct alterations in the proximal versus distal enhancer regions

Susan B. Ward[1], Gabriela Hernandez-Hoyos[1,2], Fei Chen[1], Marian Waterman[3], Raymond Reeves[4] and Ellen V. Rothenberg[1,*]

[1]Division of Biology MC156-29, California Institute of Technology, Pasadena, CA 91125, USA, [2]Stowers Institute for Medical Research, 4949 Rockhill Road, Kansas City, MO 64110, USA, [3]Department of Microbiology and Molecular Genetics, University of California, Irvine, CA 92697-4025, USA and [4]Department of Biochemistry and Biophysics, Washington State University, Pullman, WA 99164-4660, USA

ABSTRACT

Known transcription factor–DNA interactions in the minimal enhancer of the murine interleukin-2 gene (*IL-2*) do not easily explain the T cell specificity of *IL-2* regulation. To seek additional determinants of cell type specificity, *in vivo* methodologies were employed to examine chromatin structure 5′ and 3′ of the 300 bp *IL-2* proximal promoter/enhancer region. Restriction enzyme accessibility revealed that until stimulation the *IL-2* proximal promoter/enhancer exists in a closed conformation in resting T and non-T cells alike. Within this promoter region, DMS and DNase I genomic footprinting also showed no tissue-specific differences prior to stimulation. However, DNase I footprinting of the distal –600 to –300 bp region revealed multiple tissue-specific and stimulation-independent DNase I hypersensitive sites. Gel shift assays detected T cell-specific complexes binding within this region, which include TCF/LEF or HMG family and probable Oct family components. Upon stimulation, new DNase I hypersensitive sites appeared in both the proximal and distal enhancer regions, implying that there may be a functional interaction between these two domains. These studies indicate that a region outside the established *IL-2* minimal enhancer may serve as a stable nucleation site for tissue-specific factors and as a potential initiation site for activation-dependent chromatin remodeling.

INTRODUCTION

Expression of the interleukin-2 gene (*IL-2*) is highly tissue restricted and activation dependent. The molecular basis for this restriction is not yet known. The minimal DNA regulatory elements that control *IL-2* expression in T cells were initially mapped to the first 300 bp proximal of the start site (1–3).

Analysis of this 300 bp promoter/enhancer region using both *in vitro* characterization of specific transcription factor–DNA binding interactions as well as transient expression assays led to a number of important insights into the nature of *IL-2* gene regulation (for reviews see 4–6). First, the minimal promoter/enhancer region contains binding sites for both tissue-restricted and ubiquitously expressed transcription factors. *In vitro* DNA binding assays indicate that a subset of these factors can only interact with their binding sites upon stimulation, while others can bind without prior activation (7). Factors implicated in *IL-2* regulation through interactions in the proximal enhancer include the stimulation-dependent factors NF-AT, NF-κB and AP-1 and the constitutive factor Oct-1 (8–16). Most importantly, however, no tissue-specific positive or negative factor(s) has yet been identified which interacts with the *IL-2* promoter and which explains the restriction of *IL-2* gene expression to T cells.

In the light of this, it is interesting to determine what may in fact limit the expression of *IL-2* in non-*IL-2* producing cell types. Although at least some promoter/enhancer binding factors are present in the nuclei of non-T cells, *in vivo* footprinting analysis using DMS modification revealed that no factors actually interact with the minimal promoter in unstimulated T or non-T cells (17). These *in vivo* assays illustrated that, in its native chromosomal context, binding to the *IL-2* proximal 300 bp region is strictly coordinated and probably cooperative (17,18). The current model implies that no factors bind stably to the *IL-2* promoter region unless all factors are present and are competent to bind. The relatively weak, non-consensus nature of most transcription factor binding sites in the *IL-2* promoter may promote this type of cooperative interaction (19,20). At face value, this might reflect a requirement for highly stereospecific contacts among the transcription factors themselves, such that T cell specificity might emerge from the precise combination of factors which must be present simultaneously. However, there is increasing evidence which indicates that the type and relative importance of factors that interact with this minimal promoter/enhancer region may in fact be quite diverse, depending on the cellular context (21–26). These results

*To whom correspondence should be addressed. Tel: +1 626 395 4992; Fax: +1 626 449 0756; Email: evroth@cco.caltech.edu

imply that there is a certain amount of plasticity in the interaction of different factors with this essential promoter/enhancer region. Thus it is unlikely that a unique combination of factors interacting at this promoter/enhancer is responsible for T cell-specific *IL-2* expression. If tissue specificity does not result from a unique factor or combination of factors binding to the minimal enhancer, then its source must be sought elsewhere.

An important clue to a potential mechanism of regulation was provided by Siebenlist *et al.* (27). These investigators reported the presence of several DNase I hypersensitive (HS) sites within ~300 bp 5′ of the start site of the human *IL-2* gene. DNase I HS sites are hallmarks of alterations in chromatin structure and are generally representative of important regulatory regions (28,29). The ability of chromatin to restrict the binding of specific transcription factors and thereby influence gene activation is now well appreciated (30–36). There is also a growing base of evidence that discrete regions important for establishing chromatin organization exist in several genes and that these characteristically make a substantial contribution to gene expression (37,38). In addition, the presence of lineage-specific DNase I HS sites often ensures differential responses to dynamic changes in the environment (39). The early findings in the human *IL-2* gene imply that there is a potential role of chromatin structure in *IL-2* gene regulation.

In this paper we used *in vivo* DMS and DNase I footprinting to map protein–DNA contacts and alterations in chromatin at single base resolution, from –600 to +400 bp relative to the murine *IL-2* start site. We show that within the murine *IL-2* gene there are indeed several tissue-specific DNase I HS sites. In contrast to previous studies, though, we find that tissue-specific stimulation-independent DNase I HS residues are confined to the –600 to –300 bp distal region and are therefore separate from the proximal enhancer itself. The precise location of these DNase I HS residues defines two functionally distinct domains within the *IL-2* promoter. In addition, further increases in DNase I HS sites upon stimulation indicate that conformational changes extend into the proximal promoter region and may facilitate gene activation. Finally, we provide evidence for tissue-specific protein–DNA interactions within the distal DNase I HS region.

The data suggest that tissue-specific transcriptional regulation of the *IL-2* gene is mediated by factors which influence the chromatin structure of the *IL-2* locus in a tissue-specific manner and which thereby facilitate the binding of stimulation-dependent transcription factors that are otherwise excluded by generally repressive chromatin. This facilitation results ultimately in polymerase loading and gene activation. One such site of chromatin regulation is present within the –600 to –300 bp region of the *IL-2* gene.

MATERIALS AND METHODS

Cell culture

EL4.E1.F4 (EL4) thymoma cells were maintained in RPMI 1640 medium supplemented with 6% FCS, 2 mM L-glutamine, 50 μM 2-mercaptoethanol and antibiotics. 32D clone 5 (32D) pre-mast cells were maintained in DMEM supplemented with 10% FCS, 20% WEHI-3B supernatant, 2 mM L-glutamine and antibiotics. 10T1/2 fibroblasts, a gift from S.Zabludoff and B.Wold, were maintained in DMEM supplemented with 10% FCS and antibiotics. Cells in suspension were stimulated for 3–5 h at 1–2 × 10^6 cells/ml with TPA and A23187 at final concentrations of 10 ng/ml and 180 nM respectively. For adherent cells, 10 cm plates were stimulated when cells were ~70–80% confluent. Cyclosporin A

(CsA) was used at a final concentration of 0.5 μg/ml and was added 10 min prior to stimulation.

Restriction endonuclease digestions in nuclei

Nuclei from cells that were either stimulated or unstimulated were isolated and digested with *Dra*I according to Boyes and Felsenfeld (40). Briefly, 2 × 10^7 cells were washed with PBS and resuspended in 1 ml buffer A (0.34 M sucrose, 10 mM HEPES, pH 8.0, 60 mM KCl, 2 mM EDTA, 0.5 mM EGTA, 1.5 mM dithiothreitol, 0.5 mM spermine, 0.15 mM spermidine) plus 0.5% NP-40. After pelleting, nuclei were washed once in buffer A without NP-40 and resuspended in 500 μl buffer F (100 mM NaCl, 50 mM Tris–HCl, pH 8.0, 5 mM MgCl$_2$, 0.1 mM EGTA, 1 mM 2-mercaptoethanol). *Dra*I (10 U/μl; Boehringer Mannheim) was added to a final concentration of 200 U/ml and nuclei were incubated at 37°C for 1 h. The reaction was stopped by addition of EDTA to 25 mM and SDS to 0.5%. Proteinase K was added to 400 μg/ml and samples were incubated at 37°C for a minimum of 4 h. DNA was extracted twice with phenol/chloroform, once with chloroform and then precipitated with ethanol. Purified *Dra*I-digested DNA was re-digested with *Xmn*I (New England Biolabs) *in vitro* to provide an internal standard for the amount of *in vivo Dra*I digestion. Digestion products were visualized using primer extension. Briefly, 10 μg DNA digested *in vivo* with *Dra*I and *in vitro* with *Xmn*I was used in a 30 μl reaction containing extension buffer (1×: 10 mM Tris–HCl, 50 mM KCl, 3 mM MgCl$_2$, 0.05% NP-40, 0.05% Tween-20), 200 μM dNTPs, 2 pmol end-labeled primer (primer 2-6) and 2.5 U Taq DNA polymerase. PCR cycles were as follows: 1 × (94°C 4 min, 65°C 2 min, 72°C 3 min) followed by 29 × (94°C 2 min, 65°C 2 min, 72°C 3 min) and 1 × (72°C 15 min). After addition of stop solution (260 mM sodium acetate, 10 mM Tris–HCl, pH 7.5, 4 mM EDTA, 68 μg/ml yeast tRNA), samples were phenol extracted and precipitated before electrophoresing on a 6% denaturing polyacrylamide gel. The total amount of extension product in each lane is indicated by the sum of the *Xmn*I band and the *Dra*I band.

Nuclear protein extracts and EMSA

Isolation of nuclear extracts and gel shift assays were performed using a modified mini-extract protocol (41). Briefly, nuclei from stimulated or unstimulated cells were isolated after mild treatment of cells with dilute NP-40 in buffer A supplemented with 0.75 mM spermidine, 0.15 mM spermine, 10 mM Na$_2$MoO$_4$ and protease inhibitors. Nuclear factors were then isolated by incubation at 4°C in buffer C. Aliquots of 5 μg cleared nuclear extract were pre-incubated with 1 μg dI·dC before addition of radiolabeled double-stranded oligonucleotide. After incubation at 4°C, the reaction was loaded onto a 6 or 8% native polyacrylamide gel and electrophoresed at 300 V in buffer containing 0.5× TBE. For cold competitions, a 100-fold excess of unlabeled oligo was added to the binding reaction 10 min prior to addition of ^{32}P-labeled oligonucleotide probe. The LEF-1 purified protein was prepared as described (42). Purified HMG-I/Y was prepared as described (43). Samples of 20 ng each purified protein were added to the binding reaction in the presence of 0.5 μg either dI·dC or dG·dC. The oligonucleotide used in the gel shift assay that corresponds to the region from –427 to –390 in the murine *IL-2* gene is designated BC (5′-GATCCTAATCAACAAATCTAA<u>A</u>AGATTT-ATTCTTTTCATCTA-3′). The nucleotide that is also DMS-reactive in activated EL4 cells is underlined and corresponds to position

–410. Additional oligonucleotide probes that encompass the –410 region were as follows: BD, 5′-GATCCTAATCAACAAATCT-AA_A_AGATTTATTCT-3′; EC, 5′-GATCAATCTAA_A_AGATTT-ATTCT-3′; ED, 5′-GATCAATCTAA_A_AGAT-3′; FG, 5′-GATC-TTATTCTTTTCATCTA-3′; consensus octamer, 5′-GATCGAA-TGCAAATCACTAGA-3′. All double-stranded oligonucleotide probes were end-labeled using the Klenow fragment of DNA polymerase. The sequence GATC was added to each oligonucleotide to facilitate the end-labeling reaction.

In vivo DMS and DNase I footprinting

DMS treatment of both suspension and adherent cells was performed as described (44). DNase I treatment was performed as described (45) with the following modifications. For cells in suspension, cells were washed once with PBS and resuspended in DNase I digestion buffer (15 mM Tris–HCl, pH 7.5, 60 mM KCl, 15 mM NaCl, 5 mM MgCl$_2$, 0.5 mM EGTA, 300 mM sucrose, 0.05% NP-40) containing 25, 50 or 75 µg/ml DNase I (Boehringer Mannheim grade I). After 3 min at room temperature, an equal volume of 2× stop solution (50 mM EDTA, 1% SDS, 100 mM Tris–HCl, pH 8.0, 600 mM NaCl) was added. Proteinase K was added to a final concentration of 400 µg/ml and the samples were incubated at 37°C for 3 h to overnight. For adherent cells, 10 cm plates at 70–80% confluency were treated as stated above. In general, three concentrations of DNase I were used for each condition. It was necessary to titrate the DNase I in each case to obtain the best comparisons between samples. While DNase I reactivity is not sequence specific, it is influenced by relative sequence composition. The GC-richness, length of AT tracts and the width and depth of the minor groove will influence the sensitivity to DNase I digestion (46). Regions of non-reactivity seen with *in vivo* samples are also seen in the *in vitro* treated sample, indicating an inherently lower reactivity rather than a specific protection.

Purified DNase I-treated DNA was denatured by heating at 65°C for 30 min in 0.1 M NaOH, 0.5 mM EDTA. The solution was then neutralized by addition of an equal volume of 600 mM sodium acetate and precipitated with ethanol. Aliquots of 1–2 µg DNase I-treated DNA were used in ligation-mediated PCR (LM-PCR) as described (47–49). For *in vitro* treated DNA, purified genomic DNA was treated with DNase I as described above, except that ~100-fold less DNase I was used. The primers and PCR conditions are listed below. A schematic representation of where the primers are located in the murine *IL-2* gene is shown in Figure 1. Primers 2-1–2-6 and LMPCR1 and 2 were also used in Garrity *et al.* (17).

2-1, CTATCTCCTCTTGCGTTTGTCCACC, 60°C;
2-2, TGTCCACCACAACAGGCTGCTTACAGGT, 69°C;
2-3, CACCACAACAGGCTGCTTACAGGTTCAGGATG, 72°C;
2-4, GGACTTGAGGTCACTGTGAGGAGTG, 60°C;
2-5, CAAGGGTGATAGGCAGCTCTTCAGCATG, 69°C;
2-6, CAAGGGTGATAGGCAGCTCTTCAGCATGGGAG, 72°C;
1, CATCCTGAACCTGTAAGCAGCCTG T, 60°C;
2, CAGCCTGTTGTGGTGGACAAACGCAAG, 67°C;
3, CTGTTGTGGTGGACAAACGCAAGAGGAGATAG, 70°C;
4, CACTGACTGAATGGATTTAGGTGAAATC, 60°C;
5, GATTTAGGTGAAATCCCTCTTGGTCGG, 64°C;
6A, TCCCTCTTGGTCGGGGTTAGCCCACACTTAGGT, 70°C;
7, CACCAACATCCTTAGATGCAACCCT, 60°C;
8, GCAACCCTTCCTGAGAATTTGTTGGACA, 64°C;
9, CCCTTCCTGAGAATTTGTTGGACATCATACTC, 67°C;
10, CTCTGGCTAACTGTATGAAGCCATC, 60°C;

11, GAAGCCATCTATCACCCTGTGTGCA, 65°C;
12, CTATCACCCTGTGTGCAATTAGTCATTGTG, 68°C;
13, CCTAAGTGTGGGCTAACCCGA, 60°C;
14, GGCTAACCCGACCAAGAGGGA, 64°C;
15, CCAAGAGGGATTTCACCTAAATCCATTCAGTC, 66°C;
15A, AGGTAATGCTTTCTGCCACACAGGTAGACTC, 67°C;
16, GTGCTTCCGCTGTAGAGCTTG, 60°C;
17, GAGCTTGAAGTGGAGCTTGAAGTGG, 66°C;
18, GAAGTGGAGCTTGAAGTGGGTGCGCTGTTGAC, 72°C;
19, GCACCAGGAGCAGCTGTTGATG, 60°C;
20, GCTGTTGATGGACCTACAGGAGCTCC, 67°C;
21, CCTACAGGAGCTCCTTGAGCAGGATGGAGGTA, 72°C;
22, CATTAGAGCACCAGTTAAACAG, 60°C;
23, CCAGTTAAACAGAAACTCACTCACCTGC, 66°C;
24, CAGAAACTCACTCACCTGCTTGGGCAAG, 69°C;
LMPCR1, GCGGTGACCCGGGAGATCTGAATTC;
LMPCR2, GAATTCAGATC.

Detection of DNase hypersensitive sites by Southern blotting

Approximately 100×10^6 cells were washed once and resuspended in 1 ml buffer A [60 mM KCl, 15 mM NaCl, 0.66 mM MnCl$_2$, 0.1 mM EGTA, 15 mM Tris–HCl, pH 7.4, 0.3 M sucrose, 0.5 mM DTT (Boehringer), 0.1 mg/ml PMSF (Sigma), 1 µg/ml aprotinin (Boehringer)]. Cells were permeabilized by addition of 250 µl buffer A containing 150 µg/ml lysolecithin [stock, 25 mg/ml in 1:1 (v/v) chloroform/methanol; Sigma] and mixed for 30 s. Permeabilization was immediately assessed by exclusion of eosin under a phase contrast microscope using 10 µl aliquots: samples were considered permeabilized when ~95% of cells were positive for eosin; when necessary, more lysolecithin was added. The concentration of lysolecithin was diluted within <5 min by adding 4 ml buffer A with 5% glycerol and mixing carefully. Aliquots of 500 µl were prepared in 1.5 ml microcentrifuge tubes. Serial dilutions of DNase I (stock solution, 15 U/µl in 50% glycerol; Worthington) in 50 µl volumes in DNase I dilution buffer (5 mM CaCl$_2$, 0.066 mM MnCl$_2$) were added to the samples, mixed and incubated for 10 min at 37°C. The reactions were stopped by addition of 50 µl DNase stop solution (5% SDS, 100 mM EDTA). The samples were treated with 25 µg/ml RNase for 1 h and overnight with 800 µg/ml proteinase K, both at 37°C, and extracted with phenol/chloroform and precipitated with isopropanol.

Samples of 20–30 µg DNA were digested with *Xba*I, electrophoresed in agarose gels and blotted. Blots were prehybridized with 100 µg/ml salmon sperm DNA and probed with radioactively labeled probes (Prime-a-Gene labeling kit; Promega) in 0.5 M NaHPO$_4$, pH 7.4, 1 mM EDTA, 7% SDS at 65°C. Washes were carried out in 0.5× SSC, 0.1% SDS at 65°C. The *IL-2* probe used was a 784 bp *Acc*I–*Xba*I second intron fragment that spans from +1877 to +2661 from the transcription initiation site.

RESULTS

The minimal enhancer region of *IL-2* is equally inaccessible in resting T and non-T cells alike and is remodeled only in stimulated T cells

The central question addressed in this work is whether the unique ability of T cells to express the *IL-2* gene is associated with any pre-existing T cell-specific features, i.e. with any protein–DNA interactions at the *IL-2* locus that may be maintained even in the absence of inducing signals. Our previous studies, which

A

-730

-530

-410

CACCCd   NFATd   OCTd

-330

TGGGC   NFkB   AP-1d   ATGG   CD28RE   AP-1p

NFATp   OAP-40/OCT   CACCCp   TATA-2

-140

TATA-1   +1   I

+61

II

+261

B

Figure 1. Map of the murine *IL-2* gene: murine and human sequence conservation and location of primers used in this study. (**A**) Extensive homology between the murine and the human *IL-2* genes extends beyond the 300 bp minimal enhancer and into the coding sequence. The murine sequence is shown on the top line and the human sequence is on the bottom line. Exons 1 and 2 are underlined and are indicated by I and II respectively. The binding sites for known transcription factors are underlined in the murine sequence and labeled. Notice that the distal region from –600 to –300 is as well conserved as the minimal enhancer region from –300 to +1. Sequence comparisons were made using the Bestfit program (GCG). The published murine *IL-2* sequence does not extend 3′ of the *Eco*RI site at +426. (**B**) Schematic overview of the *IL-2* gene and the *in vivo* footprinting primers used in this study. Three primers are listed under each arrow since the LM-PCR relies on the use of three overlapping primers to achieve specificity. Arrows indicate the direction of extension of each primer set. Arrows pointing downstream assay events occurring on the non-coding strand, while those pointing upstream detect interactions on the coding strand. The location of the *Dra*I site (–169 to –164) within the minimal enhancer is also indicated.

examined the interaction of transcription factors with the minimal enhancer region of the *IL-2* gene, showed that distinct DMS footprints could be detected only in activated T cells (17,18). Both resting T cells and non-T cells showed a lack of any DMS footprints in this region. Because DMS does not detect histone–DNA interactions, however, we could not conclude whether the DNA in T and non-T cells was equally 'free' of all protein–DNA contacts or, alternatively, if in one case it was actively blocked by an association with repressive chromatin.

To compare the degrees to which the *IL-2* minimal enhancer might be occluded in non-T cells, unstimulated T cells and stimulated T cells, we measured the accessibility, in intact nuclei, of a *Dra*I restriction site located in the minimal enhancer (–169 to –164; see Fig. 1). This site is not footprinted with DMS and is not associated with known transcription factor binding. If the DNA molecule was digested *in vivo* by the addition of *Dra*I enzyme, then it would yield a shorter primer extension product (using primer 2-6; see Fig. 1) than if it remained intact until extraction and cleavage *in vitro* with *Xmn*I. By comparing the amount of *Dra*I product with the total yield of the amplified extension product from this region, as determined by the combined yield of the *Dra*I product and the larger *Xmn*I internal control product, it is possible to measure the relative accessibility of this *Dra*I site in different cell types.

Figure 2 shows that the *Dra*I site becomes substantially accessible to cleavage only in activated EL4 T cells. In the sample prepared from activated EL4 T cells (lane 2, Fig. 2), the *Dra*I product represents >50% of the total extension product. In non-T cells (32D pre-mast cells; lane 4), the *Dra*I site is substantially less accessible even upon activation. However, the *Dra*I site is almost equally inaccessible in resting EL4 T cells and in T cells stimulated in the presence of CsA, which blocks activation of selected transcription factors (lanes 1 and 3), as it is in the non-T cell 32D cell line. Thus, occlusion of this central region of the minimal enhancer occurs in T and non-T cells alike, implying that there is no special mechanism in T cells which keeps these promoter-proximal sequences accessible when the *IL-2* gene is not transcribed.

A strategy for seeking sites of cell type-specific stable protein–DNA interactions

To test whether specific protein–DNA interactions outside the proximal promoter/enhancer region could distinguish the state of the *IL-2* locus in T and non-T cells independently of stimulation, we investigated sequences from –600 to +400, extending from ~300 bp upstream to 400 bp downstream of the minimal enhancer. Sequences up to –600 had previously been shown to be highly conserved between the murine and human *IL-2* genes (50) and further investigation showed that this conservation extended downstream as well (Fig. 1).

We used several footprinting reagents to monitor different kinds of protein–DNA interactions in the *IL-2* gene. *In vivo* DMS footprinting was used to assay for protein interactions with G residues in the major groove of the DNA helix, while *in vivo* DNase I footprinting was used to assay minor groove interactions. High resolution DNase I analysis, as used here, can locate DNA distortions at borders of transcription factor binding sites and/or alterations in tertiary structure caused by protein-induced DNA bending. Since several candidate T cell-specific transcription factors bind in the minor groove (TCF-1 and Sox4) and may bend
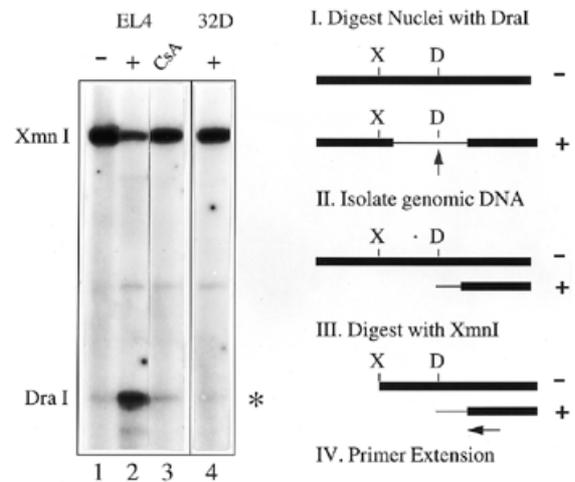

Figure 2. The *IL-2* minimal enhancer undergoes chromatin remodeling upon stimulation as shown by *in vivo* restriction enzyme accessibility. The figure shows the tissue-specific increase in accessibility to digestion of a *Dra*I site within the minimal enhancer upon gene activation. Intact nuclei isolated from stimulated or unstimulated cells were digested with *Dra*I. Genomic DNA was then extracted and digested with *Xmn*I to provide an internal standard. The extent of digestion at the *Dra*I and *Xmn*I sites was compared by primer extension using an end-labeled primer (primer 2-6). –, nuclei from unstimulated cells; +, nuclei from stimulated cells; +CsA, nuclei from cells stimulated in the presence of cyclosporin A. EL4 thymoma cells can express *IL-2* when activated, while 32D pre-mast cells cannot. The *Xmn*I product, an *in vitro* digested internal control, allows quantitation of all the molecules that were not cleaved *in vivo* with *Dra*I. The sum of the intensities of the *Xmn*I and *Dra*I bands equals the total amount of primer extension product in each sample. An increasing amount of *Dra*I product as a fraction of the total intensity is a measure of the accessibility of this locus. This *Dra*I site does not itself correspond to any known site of transcription factor binding as determined by DMS footprinting (17).

DNA, it was important to include the *in vivo* DNase I footprinting in our analysis.

These approaches revealed one major domain of DNA distortions and protein–DNA interactions that are cell type specific in the absence of activation. The major sites where we detect features of each kind are summarized in Figure 3 and are discussed below.

A novel domain of cell type-specific DNase I hypersensitivity upstream of the minimal enhancer

By comparing the DNase I footprints in resting EL4 T cells with those obtained from DNase I treatment of purified (naked) genomic DNA, a region of the *IL-2* regulatory sequence was identified that contained HS residues even in the absence of stimulation (6). This region did not overlap with the minimal enhancer, but was mapped in the current study to a discrete span of ~260 bp from –313 to –570. Figure 4 presents representative footprints of this distal region, with the non-coding strand in Figure 4A and B and the coding strand in Figure 4C and D. Comparison of the naked DNA digestion pattern (N) with the *in vivo* footprint from unstimulated T cells (–) reveals a number of individual bases that are HS in resting T cells on both the non-coding and coding strands (marked by arrows with asterisks in Fig. 4 and by inverted triangles in Fig. 3). In the regions from –313 to –361 and from –500 to –570, these HS sites occur primarily on the non-coding strand (Fig. 3 and also Fig. 4A and
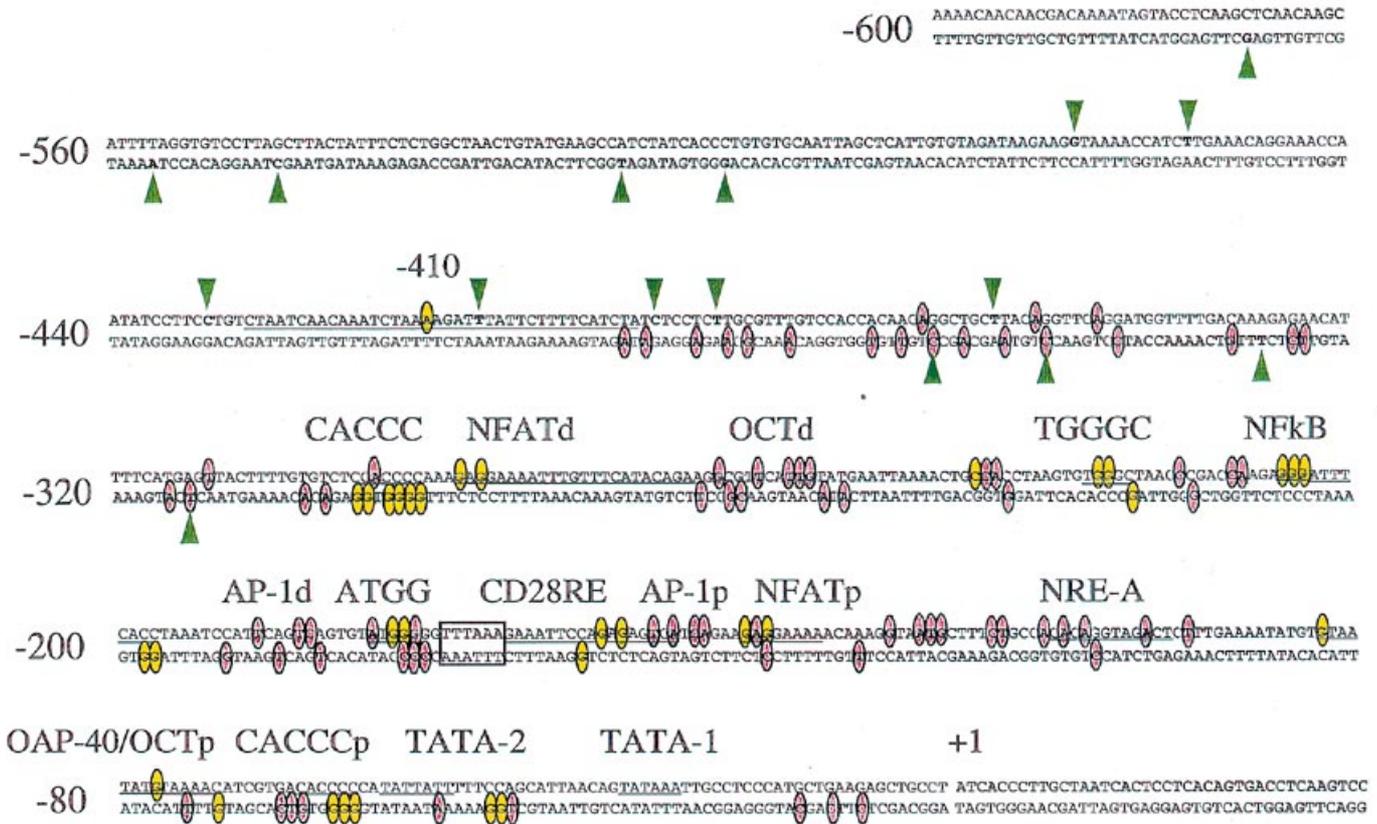
Figure 3. Summary of basal and stimulation-dependent DNase I HS sites and DMS footprints in the –600 to +40 region of the *IL-2* gene in EL4 cells. This figure represents data from Figures 4 and 6A, references 17 and 18 and unpublished data and illustrates the different domains of DNase I reactivity in the *IL-2* gene. Marked sites are those which appeared in multiple analyses of independent samples. No reproducible sites were found in exons 1 and 2 or in intron 1. Green inverted triangles indicate DNase I HS residues present in resting EL4 cells. Red ovals indicate DNase I HS residues that appear only upon stimulation. Yellow ovals indicate DMS-reactive residues, all of which are also stimulation dependent (17; this manuscript). The *Dra*I restriction site is boxed. Notice that tissue-specific HS sites present in resting EL4 cells are restricted to the distal region (–313 to –570), while activation-dependent HS residues are located within the promoter-proximal (–300 to +1) region and extend from the –9 position to position –391, which flanks a DMS-reactive site in the upstream region. No additional HS sites were induced by stimulation in the transcribed region between +1 and +426.

B). From –360 to –467, however, the HS sites are concentrated on the coding strand (Fig. 3 and also Fig. 4C and D).

Parallel analyses of footprints in 32D pre-mast cells and in 10T1/2 fibroblasts showed that none of the HS sites found in resting EL4 T cells could be detected in resting or stimulated non-T cells, as we have previously reported (6; data not shown). Furthermore, the cell type specificity of the DNase hypersensitivity around –400 was demonstrable at the level of Southern blotting, as shown in Figure 5. Here both stimulated and unstimulated EL4 cells show a well-defined HS region that can be mapped with reference to the *Xba*I sites at –2000 and within the second intron of the *IL-2* gene (Fig. 5, arrowheads). The DNase I cleavages that yield 3.0–3.2 kb fragments (upper arrowheads) correspond to the region from about –350 to –550 with respect to the transcriptional start site. While a second HS site (lower arrowhead) is also seen around the start site itself, no additional HS sites are seen between about –600 and the *Xba*I site at –2000. In 32D and 10T1/2 cells, however, no HS sites are seen anywhere within the *Xba*I fragment.

These results support the conclusion that there are cell type-specific differences in chromatin structure prior to stimulation in the region from –313 to –570 (6; data not shown). A second possible site of interaction prior to stimulation is the promoter itself, based on the Southern blotting analysis. Some of our *in vivo*

footprinting experiments have also suggested protection of the TATA boxes with HS sites at –9 and –12 prior to stimulation, although the data are inconclusive (data not shown; but see 51). In contrast to the dramatic tissue-specific and stimulation-independent DNase I HS sites found in the distal region, no cell type-specific marking features were found in the proximal enhancer or the transcribed region (Fig. 3 and data not shown).

DNase I hypersensitive sites in the distal region are stable or enhanced in activated T cells

The DNase I HS sites seen in resting T cells (Fig. 4, lanes –) are not associated with repression of the *IL-2* gene, since they are equally or more DNase I sensitive in activated T cells (+) (Fig. 4, arrows with asterisks). In addition, activation leads to further alteration of the DNA in this region, since additional sites become hypersensitive in activated T cells, as indicated in Figure 4 by arrows with circles and by red ovals in Figure 3. These new HS residues form a continuum with bases in the proximal enhancer region and appear to 'link' the distal and proximal regions. For example, multiple residues from –350 to –300 become HS only upon stimulation (Fig. 4A and C, arrows with circles). Analysis of the region upstream to –500 and downstream of the promoter
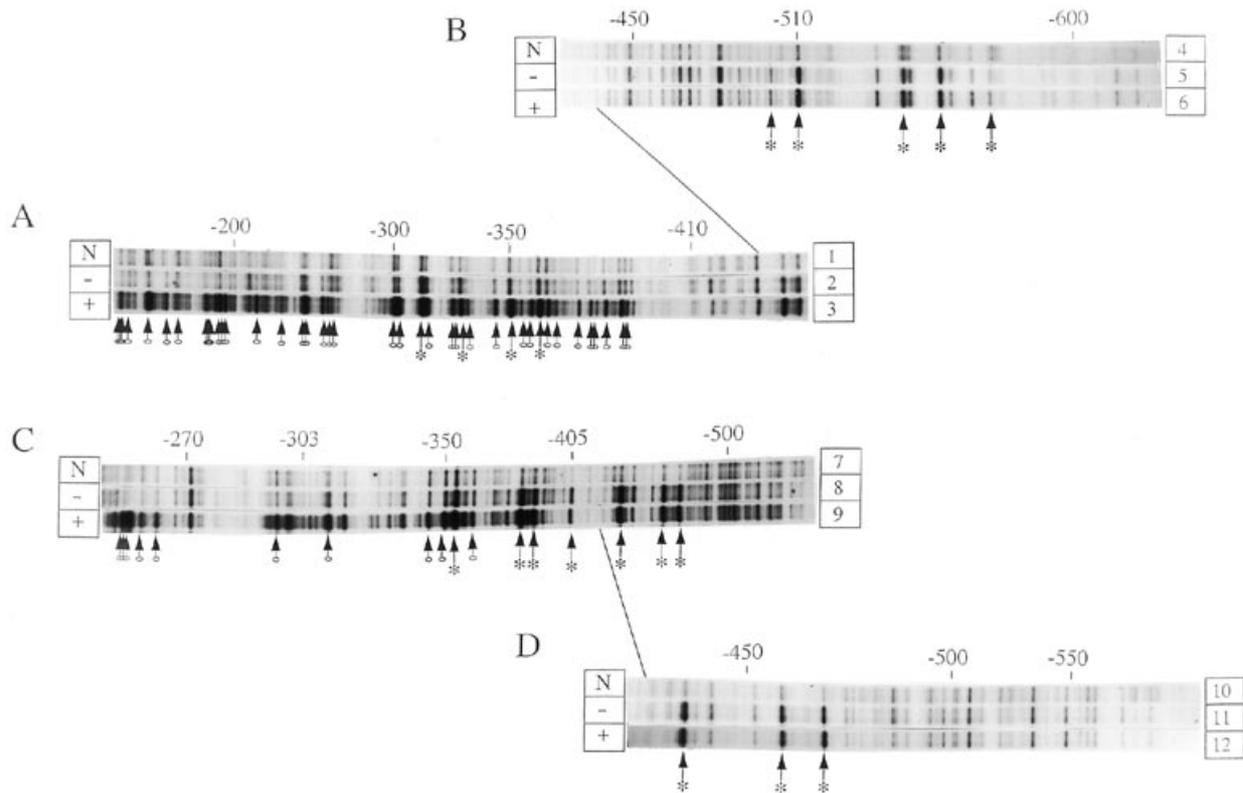
Figure 4. DNase I HS sites are present in the upstream region in resting EL4 cells. To analyze changes in chromatin structure at the *IL-2* locus, intact EL4 cells were treated briefly with DNase I after incubation with or without stimulation. *In vivo* sensitivity to DNase I was assayed by genomic footprinting using ligation-mediated PCR (LM-PCR). HS residues are defined as those LM-PCR products that exhibit higher relative intensity in stimulated cells than in unstimulated cells or higher relative intensity in unstimulated cells than in naked DNA digested *in vitro*. (**A** and **B**) *In vivo* DNase I footprinting of the non-coding strand with primers 7–9, extending from –630 to –430 (B), or primers 10–12, extending from –480 to –150 (A). (**C** and **D**) *In vivo* DNase I footprinting of the coding strand with primers 4, 5 and 6A, extending from –240 to –530 (C), or primers 1–3, extending from –410 to –600 (D). N, purified DNA treated with DNase I *in vitro*; –, unstimulated cells; +, stimulated cells. Arrows with circles indicate HS residues that are sensitive upon stimulation. Arrows with asterisks represent HS residues that are present in unstimulated EL4 cells. Lines orient one region of a gel to the same position on the adjacent gel. All lanes were loaded so as to match the intensity of those bands that were not affected by stimulation, based on multiple LM-PCR analyses extending across regions affected and unaffected by stimulation (data not shown). A portion of this composite from –300 to –400 was also included in a previous composite (6).
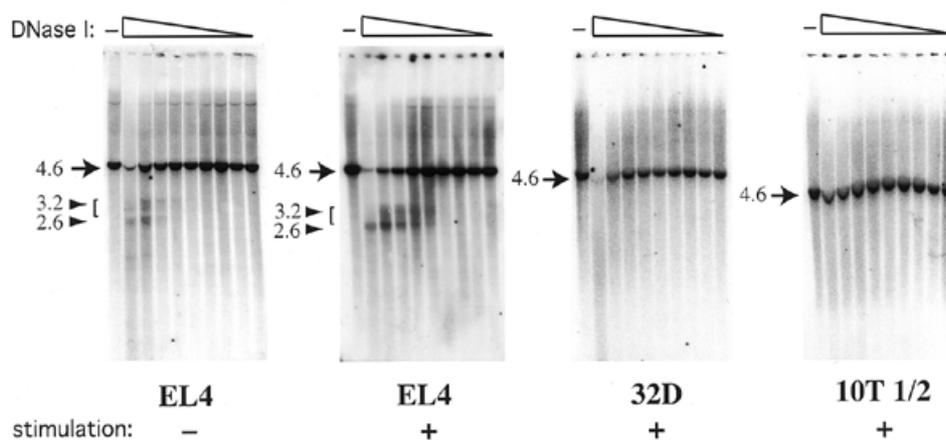

Figure 5. DNase I HS sites in the 5′-flanking region of the *IL-2* gene in *IL-2*-expressing cells only. Where indicated, cells were stimulated with TPA and A23187 for 4 h. Cells were treated with serial 2-fold dilutions of DNase I, starting at 75 U/ml for EL4 and 32D cells and at 1200 U/ml for 10T1/2 cells. DNA from permeabilized and DNase I-treated EL4, 32D and 10T1/2 cells was extracted, digested with *Xba*I and fractionated in 0.8% agarose gels. The gels were blotted and probed with a 784 bp *Acc*I–*Xba*I second intron fragment that detects a main *Xba*I product of 4.6 kb, indicated by the arrow. HS sites, indicated by the arrowheads, were only detected in EL4 cells. Sizes of the fragments are indicated in kb. Relative DNase I concentrations used decrease from left to right, as indicated by the wedge. –, no DNase.

to +400 showed both upstream and downstream boundaries of the activation-dependent HS regions. Notably, no HS sites that were activation dependent were observed upstream of –410 nor downstream of the promoter. Thus, the basal transcriptional apparatus and the features responsible for the HS site in resting T cells appear to coincide with the end-points of the region of stimulation-dependent distortion.

Induced DNase I hypersensitivity in the minimal enhancer region correlates with transcription factor binding

When T cells were activated, the minimal enhancer region became substantially more hypersensitive at specific residues within the –9 to –300 bp region (Figs 3 and 4; data not shown). Alignment of these specific sites with those of DMS footprints (17,18; summarized in Fig. 3) showed that most of the induced HS sites lie in regions between sites of DMS footprints and may be due to indirect interactions between transcription factors [e.g. between the TGGGC and NF-κB binding sites (–217 to –211) and within the OCTd (–250), AP-1d (–185) and NRE-A (–100) sites]. Other HS sites were mapped within DMS-defined regions of protein–DNA interactions and are probably caused by direct protein–DNA interactions. These results are in good agreement with the prediction that DNase I hypersensitivity *in vivo* can be induced by local transcription factor binding and emphasize the distortion of the DNA helix that occurs during the coordinated binding of disparate transcription factors over 300 bp of the minimal enhancer. The induction of DNase I HS regions within the proximal promoter/enhancer also correlates well with the increase in *Dra*I digestion seen in Figure 2.

Minimal DMS reactivity associated with DNase I hypersensitive sites upstream of the proximal enhancer

Since the appearance of DNase I hypersensitivity in the proximal enhancer was associated with the local binding of specific transcription factors as determined by *in vivo* DMS footprinting, we also used DMS genomic footprinting to attempt to locate direct protein–DNA major groove interactions in the distal enhancer region. Figure 6A shows the DMS footprint of the coding strand from the NF-ATd site at –270 in the minimal enhancer to –470. Surprisingly, the only DMS-reactive site in this entire region was found at residue –410 and only in activated EL4 T cells (lane 6, arrow with circle). In contrast, DMS clearly detects induction-dependent protection at the NF-ATd site (lane 6, arrow). No specific DMS footprints are seen in the 32D cells (lanes 2 and 3), which also do not have DNase I HS residues in this region, or in the unstimulated EL4 T cells (lane 5), which do have DNase I HS residues. Thus, the majority of the proteins responsible for the DNase I HS sites are unlikely to contact G residues in the major groove. Inspection of the sequence around the DMS-sensitive residue showed a palindromic region centered around –410 (see Fig. 3, underlined region). This site also lies near the center of the tissue-specific DNase I HS region and borders the stimulation-dependent HS 'linker' region (Fig. 3). The DMS-sensitive residue at –410 is not a G but an A, which in general is modified 5-fold less efficiently than G residues. Since no other A residues are detected under our conditions anywhere in the 1 kb region analyzed, it is likely that stimulation causes a dramatic conformational change at this residue, such that it is now more accessible to DMS modification.
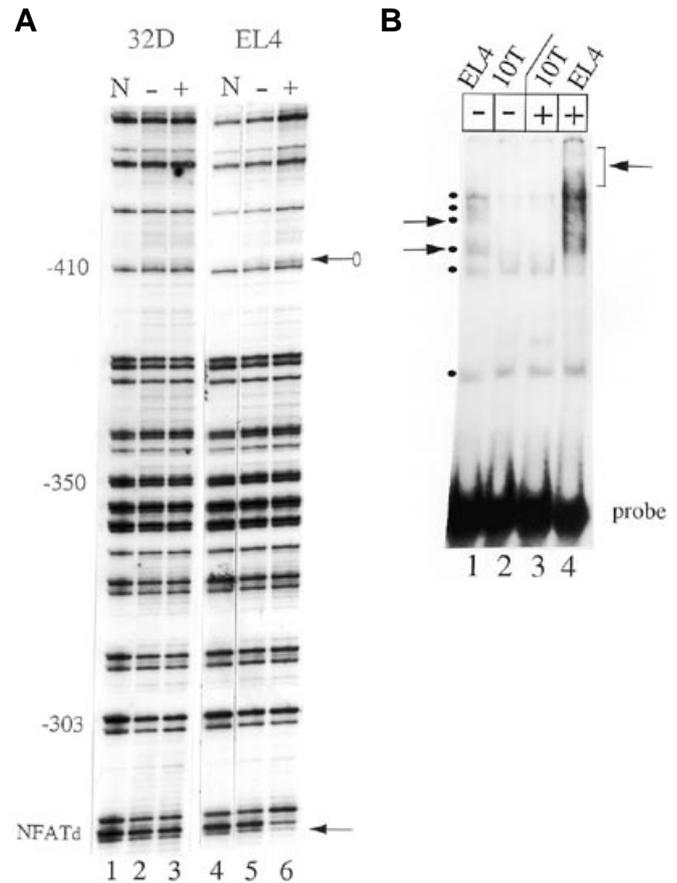

Figure 6. A discrete site in the upstream region displays both DMS sensitivity and tissue-specific protein–DNA complex formation. (**A**) Genomic footprinting of cells that were treated *in vivo* with DMS to assay for major groove protein–DNA interactions in the upstream region. Shown here is the coding strand comparison of EL4 T cells and 32D non-T cells using primers 4, 5 and 6A, which amplify from –230 to –480. Notice the lack of reactivity throughout this upstream region with the exception of a single stimulation-dependent residue at position –410. N, *in vitro* treated DNA; –, unstimulated cells; +, stimulated cells. An arrow with a circle indicates a DMS HS residue, while a plain arrow indicates a protected residue. The NFATd footprint was previously reported and provides an internal control for stimulation (17). (**B**) Tissue-specific protein–DNA interactions at the –410 site in EL4 T cells. Nuclear extracts from stimulated and unstimulated EL4 (T) and 10T1/2 (non-T) cells were incubated with a probe specific for the palindromic core of the T cell-specific stimulation-independent HS region located in the upstream region of the *IL-2* gene. Multiple shifted species are indicated by filled circles. Those complexes that are present in resting EL4 cells but not found in resting or activated 10T1/2 cells are indicated by arrows. Stimulation-dependent binding activity was only seen in extracts from activated EL4 cells and is marked by a bracket and an arrow.

A multiprotein complex binds to the distal –410 site associated with T cell-specific DMS footprints

To determine whether any protein–DNA complexes are associated with the DMS-sensitive site at position –410, we used a 37 bp DNA oligonucleotide corresponding to this region for electrophoretic mobility shift assays. As shown in Figure 6B, T cell-specific protein–DNA complexes were apparent before and after gene activation (arrows in Fig. 6B, compare lanes 1 and 2). In addition, a shift towards higher molecular weight protein–DNA complexes is seen using extracts isolated from activated T cells, suggesting that with activation, additional factors interact with this site (brackets in
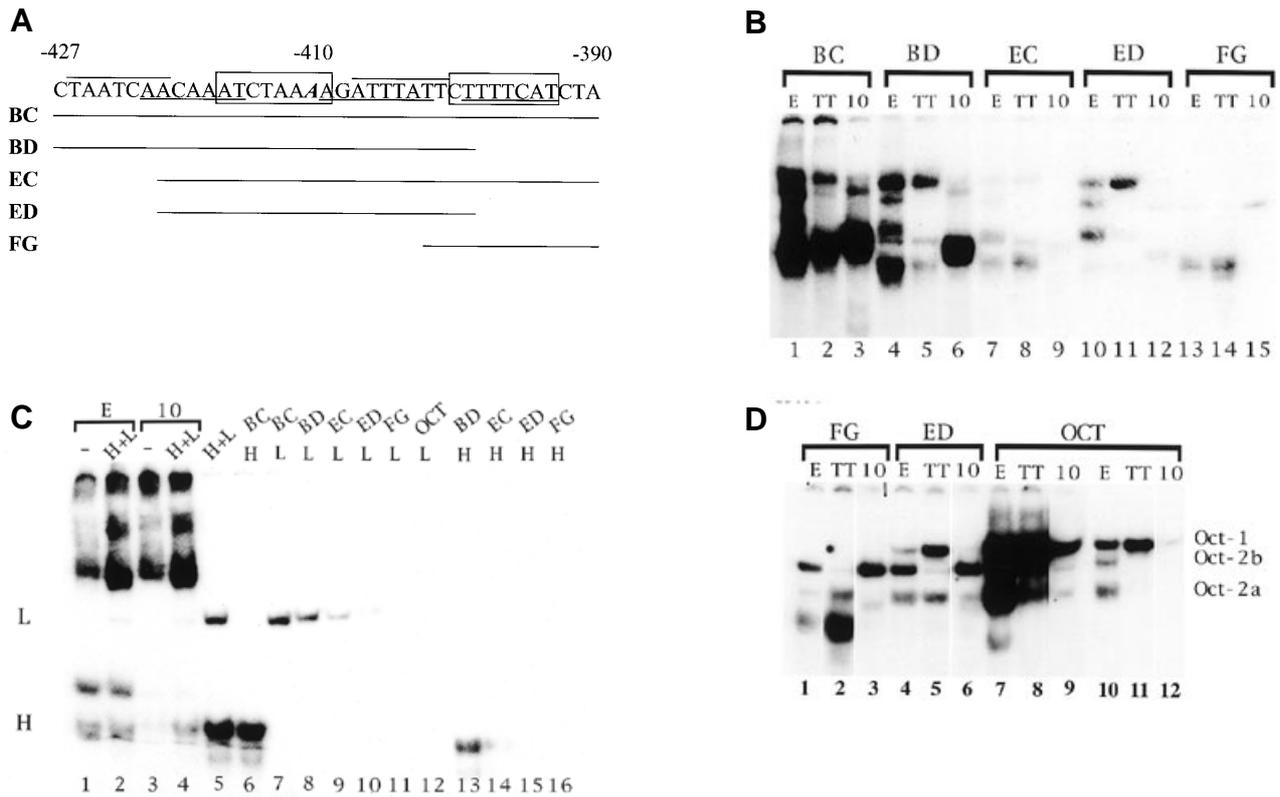
Figure 7. A complex array of factors interacts at the –410 site: potential roles for HMG and octamer factors. (**A**) Location of probes used to map factors which bind to the –410 site. Potential octamer binding sites are boxed, while potential HMG binding sites are over- or underlined. The DMS HS A residue is in italic. The regions included in different –410 site probes are indicated by lines drawn below the sequence. The exact sequence of each probe is listed in Materials and Methods. (**B**) Flanking regions of the –410 site are important for binding of factors in nuclear extracts of unstimulated cells. Deletion mapping using the probes diagrammed in (A) indicates that both the 5′ and 3′ portions of the –410 region influence factor binding. These binding assays utilized dI·dC as non-specific competitor. All samples were electrophoresed on 8% non-denaturing gels. E, EL4 (T cell) extract; TT, total thymocyte (T lineage) extract; 10, 10T1/2 (non-T) extract. The identity of the labeled probe used in each reaction is listed above the lanes. (**C**) Purified LEF-1 and HMG-I/Y bind to the –410 region and form higher order complexes with nuclear extracts. Purified LEF-1 (L) and/or purified HMG-I/Y protein (H) was added to the binding reaction in the presence or absence of nuclear extracts from unstimulated EL4 (E) or 10T1/2 (10) cells, as indicated above each lane. The BC (37 bp) probe was used in lanes 1–7 and shorter probes were used to map the sites of interaction in lanes 8–16, as indicated at the top of those lanes. The mobilities of protein–DNA complexes containing only LEF-1 (L) or HMG-I/Y (H) are indicated at the left of each panel as appropriate. These binding assays utilized dG·dC as non-specific competitor. Both LEF-1 and HMG-I/Y can bind DNA alone under these conditions (lanes 5–7), but LEF-1 binds more weakly and HMG-I/Y does not bind at all when dI·dC is used as non-specific competitor. Notice that the purified HMG-I/Y–DNA complex co-migrates with a low molecular weight shifted band in the EL4 extract. (**D**) Comparison of factors binding to –410 region octamer sites. The FG (lanes 1–3) and ED (lanes 4–6) probes contain non-consensus octamer binding sites. Factors binding to these sites are compared with factors in the same extracts that bind to a consensus octamer site (lanes 7–12). Lanes 1–9 were overexposed to illustrate the weak binding to the FG and ED probes as compared with the consensus octamer probe. Lanes 10–12 are from a lighter exposure of the same gel and serve to illustrate the presence of octamer protein in all the extracts. All reactions were performed as described in (B) and in the presence of dI·dC. E, EL4 (T cell) extract; TT, total thymocyte (T lineage) extract; 10, 10T1/2 (non-T) extract. The figure shows that the predominant species binding to the FG and ED sites in each cell extract is not necessarily the most predominant consensus octamer binding factor in the extract.

Fig. 6B, compare lanes 1, 3 and 4). The identity of the tissue-specific factors that bind to the –410 site even in the absence of *IL-2* gene activation is discussed below. These results support the possibility that the T cell-specific pattern of HS sites found at the –410 site is the result of specific protein–DNA interactions.

A potential source for tissue-specific gene marking factors

Any cell type-specific marking function would need to involve factors present in T cells prior to stimulation. To identify factors which bind the –410 site in unstimulated cells, we initially generated truncated oligonucleotide probes to map this region, as diagrammed in Figure 7A. Modified gel electrophoresis conditions were selected for these experiments to optimize resolution of the various complexes formed. Note that the AT-rich palindrome that extends, with 8/9 bp matched, from –421 to –401 gives the whole BC probe

the ability, under appropriate conditions, to form cruciform structures, which offer binding sites for structure-specific as well as sequence-specific factors, as discussed below. As shown in Figure 7A, the BD fragment (truncated at the 3′-end) retains the ability to form this cruciform structure, but the other truncated probes do not.

By comparing the complexes formed by unstimulated EL4 nuclear extracts with the different truncation variants of the –410 probes, as shown in Figure 7B, it is apparent that when the 5′- or 3′-ends are deleted from the 37 bp long probe, the complexity of the binding pattern decreases (Fig. 7B, compare lane 1 with lanes 7, 10 and 13). Removal of the 5′-end in particular (in probes EC, ED and FG) dramatically alters the binding pattern (compare lanes 1 and 4 with lanes 7, 10 and 13). This indicates that the binding of specific factors to the core of the –410 site (ED) is dependent on flanking sequences and/or on the ability to form cruciform structures.

Presence of the 3′-flanking sequence as in EC (Fig. 7B, lanes 7 and 8) appears to inhibit binding to the core region (cf. binding to ED, lanes 10 and 11, versus binding to FG, lanes 13 and 14), suggesting that there can be a complex interaction between the different factors that bind to this region. It is interesting to note that the region flanking the –410 site is conserved between the murine and human *IL-2* genes (see Fig. 1). Importantly, although the flanking sequences alter the binding, tissue-specific binding patterns are still seen when shorter probes are used in the binding assay (Fig. 7B, lanes 10–15). In addition, these experiments demonstrate several distinct complexes that are detected both in EL4 T cells and in thymocytes, but not in 10T1/2 cells (Fig. 7B, cf. lanes 4–6).

The AT-rich sequence in this region and the ability to detect extended footprints using DNase but not using DMS suggested that the complexes could contain HMG box factors, which are known to bind such sequences in the minor groove (52). HMG proteins are known to comprise important architectural components of promoter regions and can promote DNA bending and contribute regulatory information (52–55). These factors bind much more tightly to specific targets when dG·dC is used as a non-specific competitor than when dI·dC is used. This differential binding can be used as a test for the binding of such minor groove components to the –410 site. In fact, when dG·dC is used in binding assays, lower molecular weight shifted species that are not seen in the presence of dI·dC are apparent in both EL4 and thymocyte extracts (data not shown; see below). These faster migrating shifted complexes are only seen with the BC, BD and EC probes, indicating that HMG-like factors interact with the flanking sequences.

To determine whether known HMG proteins could in fact interact with this region, we performed gel shift assays using purified recombinant LEF-1, a lymphoid-specific HMG box factor (56), and HMG-I/Y, a widely expressed AT hook HMG factor (52). As shown in Figure 7C, both LEF-1 and HMG-I/Y are capable of binding to the full-length –410 probe (lanes 5–7). Deletion mapping (Fig. 7C, lanes 7–11) indicates that LEF-1 binds preferentially to the 5′-portion of the oligonucleotide. Binding by the purified HMG-I/Y protein shows an even more pronounced requirement for the 5′-portion and/or for cruciform structure (Fig. 7C, lanes 13 and 14; compare lanes 8 and 9). Slight differences in the mobilities of the complexes formed by the purified HMG-I/Y and LEF-1 proteins on the BC and BD probes (lanes 7 and 8 and lanes 6 and 13) could reflect either the binding of two complexes to the longer probes or selective binding to secondary structure features in the two probes that have slightly different effects on migration (data not shown). Interestingly, the absence of a higher order band when both purified LEF-1 and HMG-I/Y are present (Fig. 7C, lane 5) indicates that binding of the purified LEF-1 and HMG-I/Y to the –410 site may be mutually exclusive. The potential interplay between different HMG box factors at the 5′-end of the –410 region may provide an additional source of regulation (52).

A striking aspect of the LEF-1 and HMG-I/Y interactions at the –410 site is that these purified components are taken up into higher order complexes when combined with factors present in nuclear extracts (see Fig. 7C, lanes 1–4). This is shown by the decrease in free LEF-1 protein–DNA and HMG-I/Y protein–DNA complexes (compare lanes 2 and 4 with lane 5). It is also interesting to note that the intensity and composition of the nuclear extract protein–DNA complexes changes with addition of the purified LEF-1 and HMG-I/Y (see Fig. 7C, compare lanes 1 with 2 and 3 with 4). These experiments show not only that specific HMG proteins can bind to

the –410 region, but also that they can cooperate with other factors present in the nucleus to form specific complexes.

In addition to the LEF-1/HMG-I/Y binding sites, there are two non-consensus octamer binding sites in the –410 region (see Fig. 7A). Since octamer factors can interact with HMG-like factors (57) as well as other tissue-specific factors to influence gene expression (58), we wanted to determine if octamer or octamer-like factors also interact with this region. As shown in Figure 7D, complexes formed by T cell nuclear extract proteins with the sub-regions of the –410 site that contain octamer-like sites also appear to co-migrate with certain species of octamer factors (Fig. 7D, compare lanes 4 and 10 or lanes 5 and 11).

As shown in Figure 7D, the consensus octamer site binds octamer protein far better than either of the –410 octamer sites (compare lanes 1, 4 and 7 for EL4 extracts). A long exposure of this binding assay is shown (Fig. 7D, lanes 1–9) to illustrate the relatively weak binding to the ED and FG probes (lanes 1–6) as compared with octamer consensus site binding (lanes 7–9). A lighter exposure (Fig. 7D, lanes 10–12) reveals that in EL4 extracts Oct-1, Oct-2b and Oct-2a bind the consensus octamer site (Fig. 7D, lane 10; 18), while in both total thymocyte and 10T1/2 (non-T) nuclear extracts Oct-1 binds predominantly (lanes 11 and 12). The complexes binding to the ED probe, which contains the DMS-reactive A residue, are similar to those seen with the consensus octamer site when using EL4 extracts (lanes 4 and 10), implying that the factors that bind to this central site are octamer factors. Cold competition experiments verified that the corresponding complexes formed on the longer BD probe could be selectively competed with a consensus octamer binding site (data not shown). However, both the ED and FG probes tend to bind the complex resembling Oct-1 less well, relative to other species, than the consensus probe (compare lanes 1 and 2 or 4 and 5 with 10 and 11). Interestingly, while the ED probe appears to be bound by Oct-1 in the thymocyte extract, it is bound by different complexes in the 10T1/2 extract, even though both of these extracts predominantly use Oct-1 to bind the consensus octamer probe (Fig. 7D, lanes 5 and 6; compare lanes 8, 9, 11 and 12). This implies that there are tissue-specific differences in the factors that can bind to the –410 site and that there are as yet other unidentified components that interact with this region.

These results demonstrate that the –410 region is a site for several types of complex interactions. It can bind tissue-specific complexes, including some HMG proteins which could influence the architecture of the *IL-2* promoter, as well as ubiquitous factors which could potentially recruit tissue-specific factors. In addition, it appears to be composed of weak, non-consensus binding sites such that stable binding to this region is significantly influenced by the binding of neighboring factors. These features are oddly reminiscent of the proximal *IL-2* promoter and yet the –410 region is accessible prior to activation, while the proximal promoter is not. It will be interesting to determine the mechanisms whereby these different segments of the *IL-2* regulatory apparatus achieve tissue-specific occupancy and, ultimately, *IL-2* gene transcription.

DISCUSSION

While the exact nature of the proteins that can potentially bind the *IL-2* promoter may vary over the course of activation and with a variety of stimulation conditions, all factors must contend with DNA as it exists in chromatin (59,60). The results presented here provide a unique view of the chromatin status of the *IL-2* locus in the resting and activated states as well as in non-IL-2-producing cell types.

These studies offer new evidence that *IL-2* gene regulation may involve as many as three kinds of regulatory interactions. (i) Tissue-specific chromatin distortions, possibly mediated by local protein–DNA interactions, are maintained in the distal region of the *IL-2* gene in resting T cells (primarily from –570 to –313) even in the absence of activating signals. A key aspect of these distortions is that they are separated spatially from the minimal enhancer region, which is maintained in a chromatin configuration that is virtually indistinguishable between unstimulated T cells and non-T cells. (ii) Activating signals then mobilize an array of well-studied transcription factors to bind to the minimal enhancer region only in T cells (primarily from –300 to –45). The assembly of these factors induces DNase I HS sites and chromatin opening in the minimal enhancer region, while preserving or exaggerating the chromatin distortions in the upstream region. (iii) The tightly bounded propagation of new chromatin distortions upon activation, from the –410 site through the minimal enhancer region to the transcriptional start site, raises the possibility that direct physical interaction may occur between the components bound in the proximal enhancer and those bound in the distal region. The organization of these sites is consistent with a model in which *IL-2* transcription is ultimately controlled by a variety of regulatory regions and suggests a new level of complexity in *IL-2* gene regulation.

While the minimal enhancer region is altered by stimulation in a tissue-specific way, we did not detect any significant tissue-specific chromatin opening in this region prior to stimulation. Thus, in the minimal enhancer, mechanisms controlling tissue specificity cannot be separated from the molecular effectors which mediate responses to stimulation.

In contrast, the highly conserved distal domain of the *IL-2* regulatory sequence is kept in a DNase-hypersensitive chromatin configuration constitutively in cells that can make *IL-2*, even at times when *IL-2* expression is not induced. This finding suggests that the distal region has a role in regulating tissue-specific *IL-2* expression. This possibility is strengthened by the evidence for T cell-specific protein–DNA complexes within the center of the HS region from –427 to –390 and the fact that the region engaged by these T cell-specific complexes acts as an upstream boundary for the chromatin changes that accompany activation. The interaction of HMG-like factors may well play a role in establishing and/or maintaining the stimulation-independent marking of this locus as well as the activation-dependent chromatin alterations. In addition, Serfling and co-workers have suggested that Ets family proteins related to GABP can bind specifically to sites between –450 and –500 (5,61). This region is flanked by T cell-specific HS sites (see Fig. 3), although, surprisingly, we fail to see DMS footprints at these sites even with stimulation. While other interpretations clearly remain open at this stage, the most provocative possibility is that the upstream region from –390 to –427 or beyond is a domain for interaction with lineage-specific, constitutive 'marking' proteins.

Constitutively bound proteins could facilitate access to neighboring DNA sequences in chromatin in a number of ways (62–67). For example, the induction of tracts of hypersensitivity in the 'linker' region from –300 to –361, seen only upon induction, could be associated with the bending of this DNA to facilitate direct specific interactions between the constitutively bound elements upstream and the newly mobilized factors binding downstream, as shown in Figure 8. The potential implication of LEF-like factors in the T cell-specific complexes around –410 would be consistent with this, since LEF-1 is the pivot of a conformational change promoting similar interactions in the TCRα enhancer (63). This possibility is
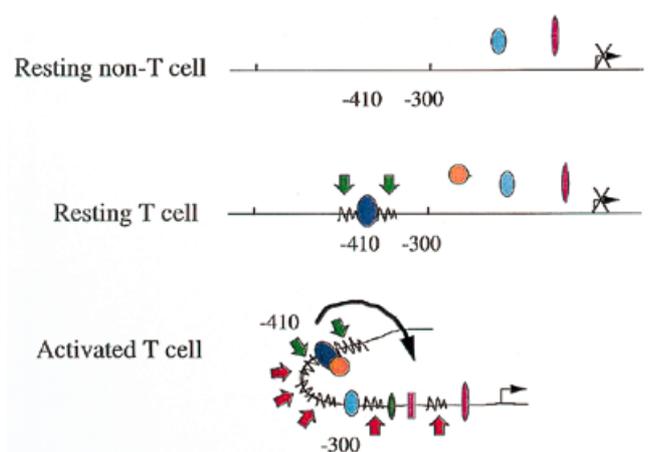

Figure 8. Model for the potential participation of the *IL-2* upstream region in tissue-specific *IL-2* gene activation. Factors which bind within the tissue-specific HS site in the upstream region participate in either the recruitment or the stabilization of other transcription factors and/or the RNA polymerase II holoenzyme to the minimal promoter/enhancer. In this way, regions outside the minimal promoter/enhancer may influence tissue-specific *IL-2* gene activation. Stimulation-dependent HS sites in the region between –300 and –410 may represent conformational changes which are depicted here as DNA bending towards the minimal enhancer. Red arrows indicate regions that become sensitive to DNase I only with gene activation. Green arrows represent regions that are hypersensitive to DNase I in resting EL4 T cells. Jagged lines represent areas of altered chromatin configuration. Circles and rectangles represent various ubiquitous, tissue-restricted and activation-dependent transcription factors.

also supported by the observation that the transcription start site demarcates a downstream boundary of the chromatin alterations that occur upon activation. Alternatively, factors that associate with the upstream region may interact with the DNA in such a way as to propagate a change in the chromatin in the direction of the minimal enhancer, which may then facilitate factor binding (68). Through any of these mechanisms or others, the ability of widely available activation factors to bind to the minimal enhancer could be subject to different thresholds in different cell types, based on the presence or absence of factors which induce chromatin distortions in the distal region.

The possibility that the conserved upstream region may play a role in chromatin organization could help explain previous equivocal evidence for its role in *IL-2* regulation. In transient transfection assays, the inclusion or exclusion of this whole region (–321 to –585) only generated a 2- to 3-fold difference in reporter gene expression (50). On the other hand, certain small deletions predicted to remove the 3′-edge of the HS region at about –360 in the human gene have indeed been reported to have very severe effects on reporter expression, even when the entire minimal enhancer is intact (69). In addition, there is also recent evidence from Serfling and colleagues that potential Ets family factor binding sites found in this region can have enhancer-like activity when multimerized out of context (5,61). It is therefore possible that the 2-fold effect on transient expression could be an underestimate of the real function of the distal region *in vivo*.

The *IL-2* gene provides a unique model to study the complexities of gene regulation and the role of chromatin in gene expression and transcription factor interactions. The mechanisms which determine and maintain specificity may ultimately take many forms, depending on the gene of interest. Single factors, combinations of factors, chromatin configuration and differences

in signaling components may all participate in the layering of regulatory controls which are necessary to specify uniqueness. The extended analysis of DNase I and DMS footprinted sites in the *IL-2* gene indicates that *IL-2* regulation is more complicated than originally thought. The results presented here suggest that conserved sequences in a relatively unstudied distal regulatory region could play a central role in establishing a chromatin configuration that is permissive for *IL-2* expression.

ACKNOWLEDGEMENTS

REFERENCES

1 Fujita,T., Shibuya,H., Ohashi,T., Yamanishi,K. and Taniguchi,T. (1986) *Cell*, **46**, 401–407.
2 Durand,D.B., Bush,M.R., Morgan,J.G., Weiss,A. and Crabtree,G.R. (1987) *J. Exp. Med.*, **165**, 395–407.
3 Crabtree,G.R. (1989) *Science*, **243**, 355–361.
4 Jain,J., Loh,C. and Rao,A. (1995) *Curr. Opin. Immunol.*, **7**, 333–342.
5 Serfling,E., Avots,A. and Neumann,M. (1995) *Biochim. Biophys. Acta*, **1263**, 181–200.
6 Rothenberg,E.V. and Ward,S.B. (1996) *Proc. Natl. Acad. Sci. USA*, **93**, 9358–9365.
7 Chen,D. and Rothenberg,E.V. (1993) *Mol. Cell. Biol.*, **13**, 228–237.
8 Serfling,E., Barthelmas,R., Pfeuffer,I., Schenk,B., Zarius,S., Swoboda,R., Mercurio,F. and Karin,M. (1989) *EMBO J.*, **8**, 465–473.
9 Shaw,J., Utz,P.J., Durand,D.B., Toole,J.J., Emmel,E.A. and Crabtree,G.R. (1988) *Science*, **241**, 202–205.
10 McCaffrey,P.G., Luo,C., Kerppola,T.K., Jain,J., Badalian,T.M., Ho,A.M., Burgeon,E., Lane,W.S., Lambert,J.N., Curran,T. *et al.* (1993) *Science*, **262**, 750–754.
11 Hoyos,B., Ballard,D.W., Bohnlein,E., Siekevitz,M. and Greene,W.C. (1989) *Science*, **244**, 457–460.
12 Kang,S., Tran,A., Grilli,M. and Lenardo,M.J. (1992) *Science*, **256**, 1452–1456.
13 Lederer,J.A., Liou,J.S., Todd,M.D., Glimcher,L.H. and Lichtman,A.H. (1994) *J. Immunol.*, **153**, 77–86.
14 Jain,J., Valge-Archer,V.E. and Rao,A. (1992) *J. Immunol.*, **148**, 1240–1250.
15 Kamps,M.P., Corcoran,L., LeBowitz,J.H. and Baltimore,D. (1990) *Mol. Cell. Biol.*, **10**, 5464–5472.
16 Pfeuffer,I., Klein-Hessling,S., Heinfling,A., Chuvpilo,S., Escher,C., Brabletz,T., Hentsch,B., Schwarzenbach,H., Mattias,P. and Serfling,E. (1994) *J. Immunol.*, **153**, 5572–5585.
17 Garrity,P.A., Chen,D., Rothenberg,E.V. and Wold,B.J. (1994) *Mol. Cell. Biol.*, **14**, 2159–2169.
18 Chen,D. and Rothenberg,E.V. (1994) *J. Exp. Med.*, **179**, 931–942.
19 Hentsch,B., Mouzaki,A., Pfeuffer,I., Rungger,D. and Serfling,E. (1992) *Nucleic Acids Res.*, **20**, 2657–2665.
20 Briegel,K., Hentsch,B., Pfeuffer,I. and Serfling,E. (1991) *Nucleic Acids Res.*, **19**, 5929–5936.
21 Mouzaki,A., Serfling,E. and Zubler,R.H. (1995) *Eur. J. Immunol.*, **25**, 2177–2182.
22 Hughes,C.C.W. and Pober,J.S. (1996) *J. Biol. Chem.*, **271**, 5369–5377.
23 Rooney,J.W., Sun,Y.-L., Glimcher,L.H. and Hoey,T. (1995) *Mol. Cell. Biol.*, **15**, 6299–6310.
24 Skerka,C., Decker,E.L. and Zipfel,P.F. (1995) *J. Biol. Chem.*, **270**, 22500–22506.
25 Civil,A., Bakker,A., Rensink,I., Doerre,S., Aarden,L.A. and Verweij,C.L. (1996) *J. Biol. Chem.*, **271**, 8321–8327.
26 Thompson,C.B., Wang,C., Ho,I., Bohjanen,P.R., Petryniak,B., June,C.H., Miesfeldt,S., Zhang,L., Nabel,G.J., Karpinski,B. *et al.* (1992) *Mol. Cell. Biol.*, **12**, 1043–1053.
27 Siebenlist,U., Durand,D.B., Bressler,P., Holbrook,N.J., Norris,C.A., Kamoun,M., Kant,J.A. and Crabtree,G.R. (1986) *Mol. Cell. Biol.*, **6**, 3042–3049.
28 Elgin,S.C.R. (1988) *J. Biol. Chem.*, **263**, 19259–19262.
29 Gross,D.S. and Garrard,W.T. (1988) *Annu. Rev. Biochem.*, **57**, 159–197.
30 Felsenfeld,G. (1996) *Cell*, **86**, 13–19.
31 Kingston,R.E., Bunker,C.A. and Imbalzano,A.N. (1996) *Genes Dev.*, **10**, 905–920.
32 Workman,J.L. and Buchman,A.R. (1993) *Trends Biochem. Sci.*, **18**, 90–95.
33 Wallrath,L.L., Lu,Q., Granok,H. and Elgin,S.C.R. (1994) *BioEssays*, **16**, 165–170.
34 Milot,E., Strouboulis,J., Trimborn,T., Wijgerde,M., de Boer,E., Langeveld,A., Tan-Un,K., Vergeer,W., Yannoutsos,N., Grosveld,F. *et al.* (1996) *Cell*, **87**, 105–114..
35 Wotton,D., Flanagan,B.F. and Owen,J.J. (1989) *Proc. Natl. Acad. Sci. USA*, **86**, 4195–4199.
36 Festenstein,R., Tolaini,M., Corbella,P., Mamalaki,C., Parrington,J., Fox,M., Miliou,A., Jones,M. and Kioussis,D. (1996) *Science*, **271**, 1123–1125.
37 Archer,T.K., Lefebvre,P., Wolford,R.G. and Hager,G.L. (1992) *Science*, **255**, 1573–1576.
38 Aronow,B.J., Ebert,C.A., Valerius,M.T., Potter,S.S., Wiginton,D.A., Witte,D.P. and Hutton,J.J. (1995) *Mol. Cell. Biol.*, **15**, 1123–1135.
39 Patterton,D. and Wolffe,A.P. (1996) *Dev. Biol.*, **173**, 2–13.
40 Boyes,J. and Felsenfeld,G. (1996) *EMBO J.*, **15**, 2496–2507.
41 Tugores,A., Alonso,M.A., Sanchez-Madrid,F. and de Landazuri,M.O. (1992) *J. Immunol.*, **148**, 2300–2306.
42 Waterman,M.L. and Jones,K.A. (1990) *New Biol.*, **2**, 621–636..
43 Nissen,M.S., Langan,T.A. and Reeves,R. (1991) *J. Biol. Chem.*, **266**, 19945–19952.
44 Mueller,P.R., Garrity,P.A. and Wold,B. (1992) In *Current Protocols in Molecular Biology*. J.Wiley & Sons, NY, pp. 15.5.1–15.5.26.
45 Stewart,A.F., Reik,A. and Schutz,G. (1991) *Nucleic Acids Res.*, **19**, 3157.
46 Suck,D. (1994) *J. Mol. Recog.*, **7**, 65–70.
47 Pfeiffer,G.P., Steigerwald,S.D., Mueller,P.R., Wold,B. and Riggs,A.D. (1989) *Science*, **246**, 810–813.
48 Mueller,P.R. and Wold,B.W. (1989) *Science*, **246**, 780–786.
49 Garrity,P.A. and Wold,B.W. (1992) *Proc. Natl. Acad. Sci. USA*, **89**, 1021–1025.
50 Novak,T.J., White,P.M. and Rothenberg,E.V. (1990) *Nucleic Acids Res.*, **18**, 4523–4533.
51 Brunvand,M.W., Krumm,A. and Groudine,M. (1993) *Nucleic Acids Res.*, **21**, 4824–4829.
52 Bustin,M. and Reeves,R. (1996) *Prog. Nucleic Acid Res. Mol. Biol.*, **54**, 35–100.
53 Grosschedl,R. (1995) *Curr. Opin. Cell Biol.*, **7**, 362–370.
54 Thanos,D. and Maniatas,T. (1992) *Cell*, **71**, 777–789.
55 John,S., Reeves,R.B., Lin,J.-X., Child,R., Leiden,J.M., Thompson,C.B. and Leonard,W. (1995) *Mol. Cell. Biol.*, **15**, 1786–1796.
56 Travis,A., Amsterdam,A., Belanger,C. and Grosschedl,R. (1991) *Genes Dev.*, **5**, 880–894.
57 Zwilling,S., Konig,H. and Wirth,T. (1995) *EMBO J.*, **14**, 1198–1208.
58 Gstaiger,M., Georgiev,O., van Leeuwen,H., van der Vliet,P. and Schaffner,W. (1996) *EMBO J.*, **15**, 2781–2790.
59 Paranjape,S., Kamakaka,R.T. and Kadonaga,J.T. (1994) *Annu. Rev. Biochem.*, **63**, 265–297.
60 Felsenfeld,G. (1992) *Nature*, **355**, 219–224.
61 Avots,A., Hoffmeyer,A., Flory,E., Cimanis,A., Rapp,U.R. and Serfling,E. (1997) *Mol. Cell. Biol.*, **17**, 4381–4389.
62 Felsenfeld,G., Boyes,J., Chung,J., Clark,D. and Studitsky,V. (1996) *Proc. Natl. Acad. Sci. USA*, **93**, 9384–9388.
63 Giese,K., Kingsley,C., Kirshner,J.R. and Grosschedl,R. (1995) *Genes Dev.*, **9**, 995–1008.
64 Grosschedl,R., Giese,K. and Pagel,J. (1994) *Trends Genet.*, **10**, 94–100.
65 Polach,K.J. and Widom,J. (1995) *J. Mol. Biol.*, **254**, 130–149.
66 Varga-Weiss,P.D. and Becker,P.B. (1995) *FEBS Lett.*, **369**, 118–121.
67 Wolffe,A.P. (1994) *Trends Biochem. Sci.*, **19**, 240–244.
68 Parekh,B.S. and Hatfield,G. W. (1996) *Proc. Natl. Acad. Sci. USA*, **93**, 1173–1177.
69 Williams,T.M., Eisenberg,L., Burlein,J.E., Norris,C.A., Pancer,S., Yao,D., Burger,S., Kamoun,M. and Kant,J.A. (1988) *J. Immunol.*, **141**, 662–666.